Bellcomm

955 L'Enfant Plaza North, S.W.
Washington, D. C. 20024

B71 10008

date: October 12, 1971

to: Distribution

from: L. P. Gieseler

subject: Survey of Potential S-IVB Lunar Impact Trajectories for Apollo 16 and 17 -- Case 310

ABSTRACT

A wide variety of trajectories for the spent S-IVB stage is possible for the Apollo 16 and 17 missions. The simplest of these are the direct impact trajectories that impact the moon on the translunar leg of the trajectory as was done during Apollo flights 13 to 15. Impacts on a limited portion of the back of the moon are possible using these trajectories with only a moderate decrease in accuracy of impact location. It is also possible to design the trajectories so that the S-IVB impact is visible from the CSM in real time.

Delayed impact trajectories, in which the moon makes one or more revolutions in its orbit before S-IVB impact are also possible. Either front or back side impacts can be achieved. Delayed impact trajectories have the advantage that the seismometer can measure the impact of the S-IVB that carried it. However, these trajectories are extremely sensitive to guidance errors, and additional orbital corrections would have to be provided to make them practical.

Bellcomm

955 L'Enfant Plaza North, S.W.
Washington, D. C. 20024

date: October 12, 1971

to: Distribution

B71 10008

from: L. P. Gieseler

subject: Survey of Potential S-IVB Lunar Impact Trajectories for Apollo 16 and 17 -- Case 310

MEMORANDUM FOR FILE

I. Introduction

The spent S-IVB stages of Apollo flights 13 to 15 were targeted to impact the moon. The seismic signals from these impacts as recorded on the lunar seismometers produced a great deal of information about the moon as well as serving as a calibration for the seismometers. Similar opportunities for S-IVB impact will exist for Apollo 16 and 17. This memorandum is a report on a study of possible impact trajectories for these missions, including those that impact the back side of the moon.

A typical procedure for controlling the S-IVB trajectory to produce a lunar impact is described in References 1 and 2. A timeline taken from the references is shown in Figure 1a. The evasive maneuver shown beginning at 1 hour and 42 minutes after TLI is accomplished with the S-IVB APS, the velocity impulse (ΔV) equaling 10 fps. The LOX dump begins 2 hours and 5 minutes after TLI, and produces a ΔV of 28 fps. The APS-1 maneuver begins 2 hours and 49 minutes after TLI, and produces a ΔV of 33 fps. The ΔV for the APS-2 maneuver occurs 6 hours and 34 minutes after TLI, but was assumed to equal zero. Tracking from the earth after each maneuver is used to determine the orientation and duration of the next burn.

II. Reference Trajectory

The Apollo 16 trajectory was used in this study, but the results should also apply to Apollo 17 as they are not very mission dependent. The trajectory was obtained by making a mission simulation with parameters appropriate for Apollo 16 using BCMASP. The significant characteristics of this trajectory are:

Launch Date	March 17, 1972
Launch Time (GMT)	19 Hours, 23 Min., 24.9 Sec.
Injection Type	Pacific
Launch Azimuth	80°
Landing Site	Descartes
Landing Approach Azimuth	-91°
Sun Elevation at Landing	9°
Translunar energy per unit mass	-9,661,000 ft^2/sec^2

An unperturbed S-IVB trajectory (illustrated in Figure 1b) is taken to be the same as the reference CSM trajectory with no powered maneuvers after TLI. The state vector at TLI was used as the starting point for the S-IVB trajectory integration. Figure 1b also shows the direction of a vector pointing to the sun when the S-IVB is at periselene in the unperturbed trajectory. This vector rotates clockwise at a rate of about 12 degrees per day.

A special coordinate system was used to display the results of the computer simulations in a meaningful way. In this system the x-axis points from the earth to the moon at the time that the S-IVB reaches periselene in the unperturbed trajectory. The y-axis lies in the lunar orbital plane perpendicular to the x-axis and directed approximately in the direction of the moon's velocity vector. The z-axis completes the right-handed coordinate system. The origin is located in the earth or in the moon for geocentric or selenocentric plots, respectively.

III. Dispersion Analysis of Impact Prediction

The error in impact location was determined by making use of the information given in Reference 2, that the 3σ error after the APS-2 burn is an ellipse on the lunar surface extending ± 50 km in latitude and ± 60 km in longitude. (The Apollo 15 results have cast some doubt on the validity of these figures, but they are still useful as a comparison of one trajectory with another.) The ellipse, shown in Figure 2, was propagated backward along the trajectory and converted to equivalent ΔV's at the APS-2 point.

First a basic trajectory having an impact location of -1° latitude and -33° longitude was obtained by adjusting the ΔV at the LOX dump point, with the ΔV's for the evasive, the APS-1, and the APS-2 maneuvers all set equal to zero. This trajectory was selected because it intersected the moon's surface nearly vertically. The impact location for this trajectory is shown in the center of the ellipse of Figure 2. The ΔV at the APS-2 point was then adjusted so that the resulting trajectories impact on the circumference of the error ellipse. Three mutually orthogonal directions of the impulse were used, and are shown in Table I:

TABLE I

Symbol	Description	Magnitude
ΔV_v	Parallel to velocity vector	±.70 fps
ΔV_r	Perpendicular to velocity vector and in the plane of the orbit. Points to the right.	±2.62 fps
ΔV_h	Parallel to the momentum vector	±1.95 fps

To obtain the error ellipse for a specific trajectory the above process was reversed. Six perturbed trajectories were calculated using the above values and directions of the APS-2 ΔV. The error ellipse was then drawn through the resulting six impact locations.

IV. Possible S-IVB Trajectories

Figure 3 shows the trajectories which result when the ΔV at the LOX dump point varies from -200 to +150 fps. The direction of the ΔV vector was made parallel to the velocity vector, since, as indicated in Table I, this is approximately the direction of maximum sensitivity. A positive ΔV represents a vector pointing in the same direction as the velocity vector. The total ΔV available is estimated at ±100 fps, but the range was enlarged to cover cases for which more propellant than expected is available after TLI. The geocentric energy per unit mass varies from -12.5×10^6 ft^2/sec^2 for $\Delta V = -200$ fps to -7.3×10^6 ft^2/sec^2 for $\Delta V = +150$ fps.

Figure 3a is a large scale picture of eight translunar approach orbits (indicated as a single curve) and the post encounter trajectories. A detail of the encounter portion of the orbits is given in Figure 3b. The moon moves along an orbit shown as a dotted line in both figures. The points shown on the lunar orbit of Figure 3b indicate the positions occupied by the moon when the S-IVB is at periselene for the various ΔV's used. When $\Delta V = -200$ fps, the resulting trajectory has such a low energy that it does not reach the orbit of the moon at all, and the effect of the lunar encounter is slight. The post-encounter portion of the orbit is shown in Figure 3a as a relatively small ellipse having a period of 9.7 days. When $\Delta V = -150$ and -100 fps, the encounter trajectories extend well beyond the lunar orbit and post-encounter ellipses have periods of 13.4 and 26.0 days respectively. When $\Delta V = -50$ fps, a so-called sling-shot trajectory results, that is, one which has gained enough energy from the

encounter to become hyperbolic. When $\Delta V = 0$, the trajectory is the unperturbed one shown in Figure 1. The period of the post-encounter ellipse is 27.1 days, and the perigee distance equals about 10 earth radii.

Trajectories for which $\Delta V = 50$, 100 and 150 fps are shown in Figure 3b only. After lunar encounter, these trajectories all lie in planes which are almost perpendicular to the lunar orbital plane. They are all very eccentric with semi-minor axes of the order of 5 earth radii, and they all impact the earth on the return leg of the trajectory. Only the outward leg of the trajectories having $\Delta V = 100$ and 150 fps is shown in Figure 3b. The apogee distances for these two trajectories equals 1.36×10^9 and 1.52×10^9 ft respectively.

Figure 4 shows the same trajectories as Figure 3 but plotted using selenocentric instead of geocentric coordinates. In this coordinate system the moon occupies a fixed position at the origin, and grazing and impact trajectories are more easily visualized than in the geocentric coordinate system. Near grazing trajectories are obtained when ΔV equals 0 and -50 fps, and these have clockwise and counter-clockwise directions respectively. ΔV's outside this range result in trajectories that have greater periselene distances and are perturbed less by the moon. The selenocentric energy per unit mass increases from 3.6×10^6 to 6.4×10^6 ft^2/sec^2 when the ΔV varies from -200 to +150 fps. Figure 4b shows in detail the two grazing trajectories mentioned above, and also the trajectories which impact the moon when the ΔV has a value between -2.5 and -48 fps. Impacts on the back side of the moon occur in the range $-15 < \Delta V < -2.5$ fps. The farthest eastern longitude attainable is about 60 degrees. Additional information about these trajectories is given in Section V.

The curves of Figure 4a exhibit a greater regularity than the same trajectories shown in Figure 3. For example, the slingshot trajectory, which in Figure 3 is an entirely different type of trajectory from the ellipses shown there, appears in Figure 4a as a logical member of a family of trajectories which are deflected by the moon in increasing amounts as the distance to the moon at periselene becomes less. The reason for the lack of uniformity of the geocentric curves is that at MSI exit the velocity of the S-IVB must be added vectorially to the velocity of the moon to obtain the post-encounter state vector. The differences in the direction of the S-IVB velocity vector causes wide variations in the resultant geocentric velocity, and corresponding wide variations occur in the orbital characteristics.

V. Direct Impact Trajectories

As shown in Figure 4b, trajectories for which ΔV at the LOX dump point has a value between -2.5 and -48 fps will impact the moon. The 3σ error in the prediction of impact location for these trajectories is shown in Figure 5a. The least error in longitude is about 50 km, and occurs at -50° longitude, where the trajectory impacts the moon vertically. As expected, the error becomes very large as the trajectory approaches a grazing condition. For an impact at 180° longitude, ΔV must be reduced to -1 fps and a 3σ error in the value of ΔV may cause the trajectory to miss the moon entirely. A similar situation occurs for impact at +60°, corresponding to a ΔV of -48 fps. Impacts on the back side of the moon with longitudes between -150° and -90° are possible with a moderate decrease in impact accuracy. Back side impacts having positive (eastern) longitudes are not possible using direct impacts. The error in latitude remains relatively constant at about 60 km over the entire range of impact longitudes.

Figure 5b is similar to Figure 5a except that the nominal trajectory was caused to impact at various latitudes, instead of various longitudes as before. (This was accomplished by orienting the ΔV vector along the angular momentum vector, instead of along the velocity vector.) The 3σ error in latitude has a minimum of 60 km at zero latitude, and increases to nearly 100 km for latitudes of $\pm 70°$. The 3σ error in longitude is almost constant at 50 km.

VI. Visibility of S-IVB Impact from the CSM

Figure 6 shows the location of the CSM when the S-IVB impacts the moon for the same family of direct impact trajectories shown in Figure 4b. A simplified CSM trajectory is assumed in which the approach hyperbola is converted into a 60 x 170 nm altitude ellipse by means of a velocity impulse at LOI. No plane change is used at LOI. There are two considerations which make it desirable to have a line of sight geometry between the CSM and the S-IVB at impact:

1. The exact impact time is required for the lunar seismographs. For a front side impact this is determined from the earth by recording the time that the S-IVB transponder stops transmitting. For a back side impact the signal cannot be received on the earth after the S-IVB disappears behind the moon. However, an S-IVB signal could be detected from the CSM provided that the two objects have an unobstructed line of sight. (At the present time the CSM is not equipped to receive such a signal.)

2. There is a great lack of information about the cratering process on the moon caused by the impact of an object as large as the S-IVB. A visual observation of the actual collision between the S-IVB and the moon would be very useful in understanding the physics involved.

Referring to Figure 6, the requirements of Item 1 would be satisfied by using trajectories for which the ΔV at the LOX dump point equals -2.5 and -5.0 fps, since these impacts are within line of sight of the CSM. However, they are near grazing trajectories, and, consequently, have a large impact location error. S-IVB trajectories having ΔV's equal to -10 or -15 fps would be more satisfactory in this respect and could be used if the CSM were delayed about 15 minutes, placing the CSM approximately at A of Figure 6. This delay is easily within the capabilities of the CSM propulsion system, as simulations have shown that a 15-minute delay can be achieved by using a ΔV of about 10 fps at the first midcourse correction.

Item 2 above requires that S-IVB impact occur in daylight. From Figure 6, this means that the S-IVB ΔV must equal about -2 fps for a back side impact at -170° longitude, or about -45 fps for a front side impact at +23° longitude. Both of these trajectories are nearly grazing and have large impact location errors. The guidance accuracy would have to be increased to insure that impact occurred at the desired location. The crater formed by the S-IVB should have a diameter of about 200 feet, subtending an angle of about one minute of arc at a distance of 100 nm. This is about the limit of resolution of the naked eye, but the crater formation and accompanying dust cloud should be easily visible by using the CSM sextant which has a magnification of 28, if appropriate pointing angles could be made available to the crew.

S-IVB impact at -170° longitude has the disadvantage that it occurs just before LOI when the attitude of the CSM is determined by the requirements of the LOI burn. In addition, the crater will be in sunlight only a few hours (since the terminator rotates in a clockwise direction) and could not be photographed later in the mission. Impact at +23° longitude does not suffer from these disadvantages. For this case the CSM is about 100° or 35 minutes ahead of the impact location and must be delayed by that amount to be within line of sight of the impact location at the moment of impact. Adjusting the CSM trajectory would require a ΔV of about 25 fps at the first midcourse correction. The viewing distance would be of the order of 200 nm, but this could be reduced for better resolution by going to a circular 60 nm altitude orbit.

VII. Delayed Impact Trajectories

Figure 3a can be used to deduce the approximate value of ΔV at the LOX dump point which will result in lunar impact after one or more revolutions of the moon in its orbit. For $\Delta V = -150$ fps the period of the resulting ellipse equals 13.4 days. Since the period of the moon's orbit equals 27.3 days, the moon will be in approximately the correct position for impact after two revolutions of the S-IVB. For $\Delta V = -100$ fps the period equals 26.0 days and the moon will be in approximately the correct position after one revolution of the S-IVB. Both possibilities would result in a front side impact. For a back side impact ΔV must be changed to -85 fps, resulting in a period of 43 days, with the moon located at an angle of about 115° with the +x axis at impact. (This trajectory is not shown in Figure 3a.) When ΔV is reduced from -85 to -50 fps the period of the resulting orbit increases without limit, and a lunar impact can theoretically be obtained after any number of revolutions of the moon in its orbit. For $\Delta V = 0$ the period equals 27.1 days, and only a slight adjustment of the orbit is required to achieve a back side impact. This trajectory goes through perigee before apogee and impact. This is a desirable feature since a corrective impulse could be applied at perigee before the trajectory error becomes too large. (At perigee the tracking distance is a minimum and, therefore, the tracking error should also be a minimum.) Hardware modifications in the S-IVB would be required both for tracking purposes and for supplying the corrective impulse.

The error ellipse shown in Figure 2 is a convenient standard for the sensitivity of a trajectory to errors in the final (APS-2) correction. The delayed impact trajectories typically have error ellipses which are 30 times as sensitive in the latitude direction and 1000 times as sensitive in the longitude direction. These trajectories are not practical unless the guidance accuracy is increased a proportionate amount.

VIII. Summary and Conclusions

A computer simulation was used to determine the characteristics of S-IVB lunar impact trajectories. The simulation was arranged to apply ΔV's at the LOX dump point to vary the gross characteristics of the orbit, and at the APS-2 point to determine the 3σ error ellipse of impact prediction. This is a simplification of the actual procedure, but the results are fully applicable to the actual case.

As might be expected the greatest accuracy of impact prediction occurs with trajectories that impact the moon on the translunar leg with a vertical impact. Back side impacts can be achieved for most western longitudes with only a moderate decrease in accuracy. The relative positions of CSM and S-IVB

at S-IVB impact can be adjusted so that the impact is visible from the CSM in real time. Such an observation or photograph would yield a great deal of information about the lunar cratering process. However, the operational procedures required would be stringent as well as complex.

Delayed impact trajectories, in which the moon makes one or more revolutions in orbit between launch and S-IVB impact, have a number of interesting characteristics. However, the error involved in guiding the S-IVB to a predetermined impact location would have to be considerably reduced before these trajectories could be used.

L P Gieseler

2013-LPG-jab

L. P. Gieseler

Attachments

REFERENCES

1. "Saturn V AS-510 Launch Vehicle Operational Flight Trajectory - Lunar Impact Trajectory for July 26 and 27 1971 Launch Days," Boeing Document No. D5-15812, dated May 26, 1971, Figure 1-1 and pages 1-8 to 1-12.

2. "AS-510 Lunar Impact Operational Procedures Plan," MSFC Memorandum, dated July 6, 1971, page 13.

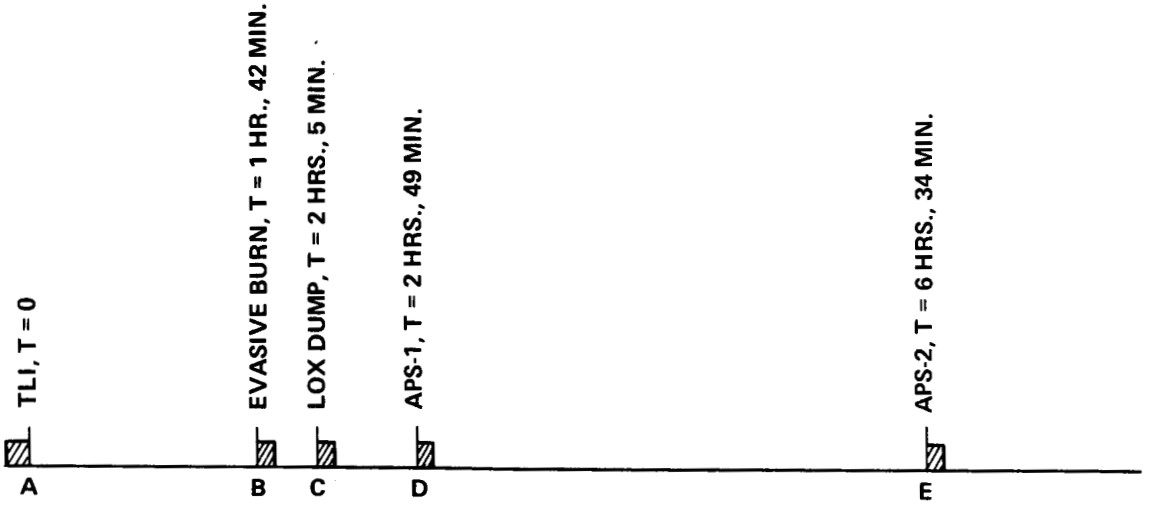

FIGURE 1a - TIME LINE FOR S-IVB MANEUVERS

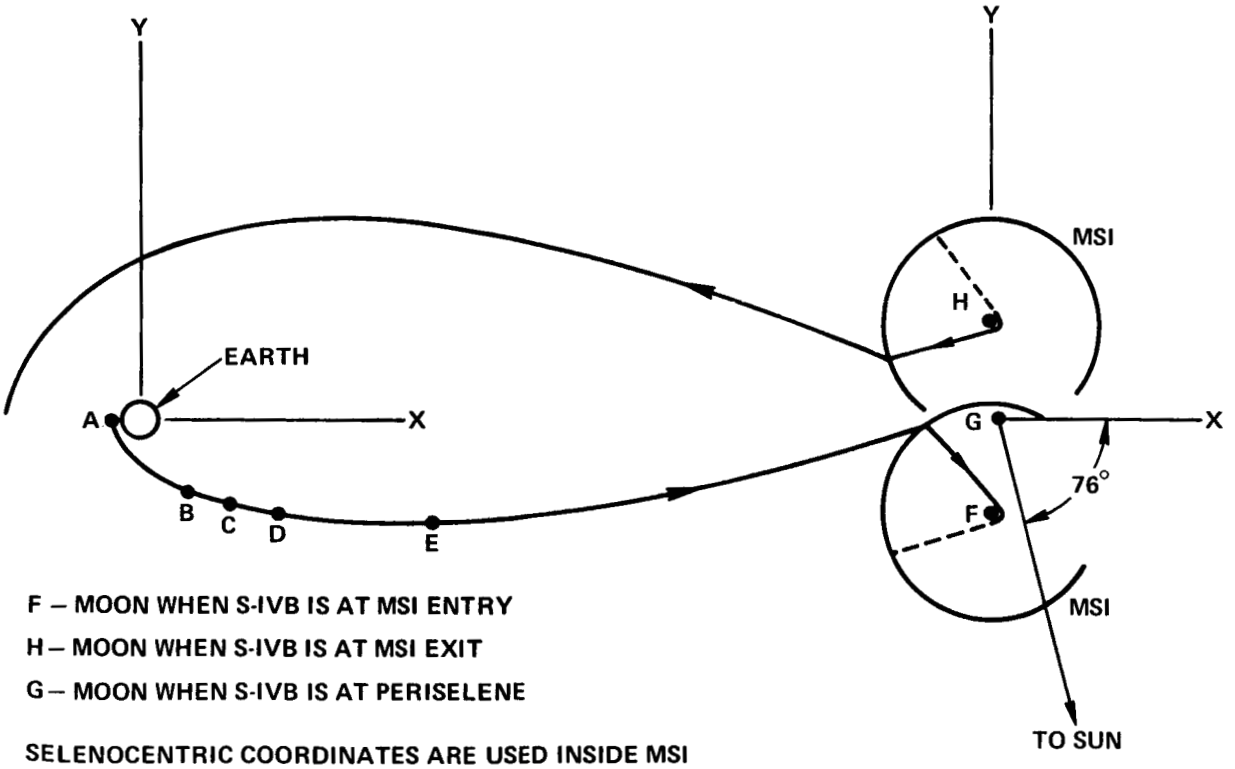

F – MOON WHEN S-IVB IS AT MSI ENTRY

H – MOON WHEN S-IVB IS AT MSI EXIT

G – MOON WHEN S-IVB IS AT PERISELENE

SELENOCENTRIC COORDINATES ARE USED INSIDE MSI

GEOCENTRIC COORDINATES ARE USED OUTSIDE MSI

FIGURE 1b - UNPERTURBED S-IVB TRAJECTORY

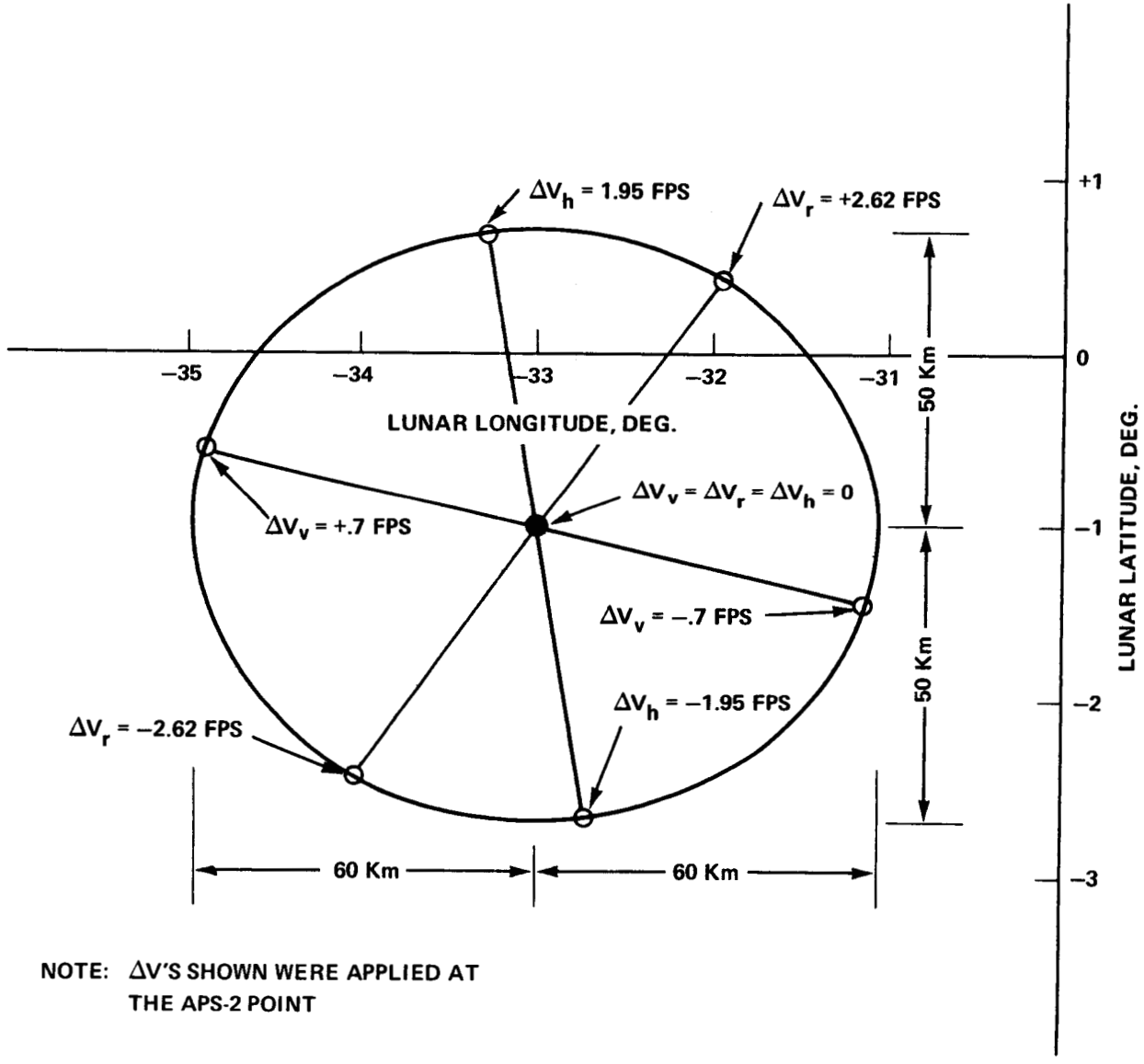

NOTE: ΔV'S SHOWN WERE APPLIED AT THE APS-2 POINT

FIGURE 2 - ERROR ELLIPSE

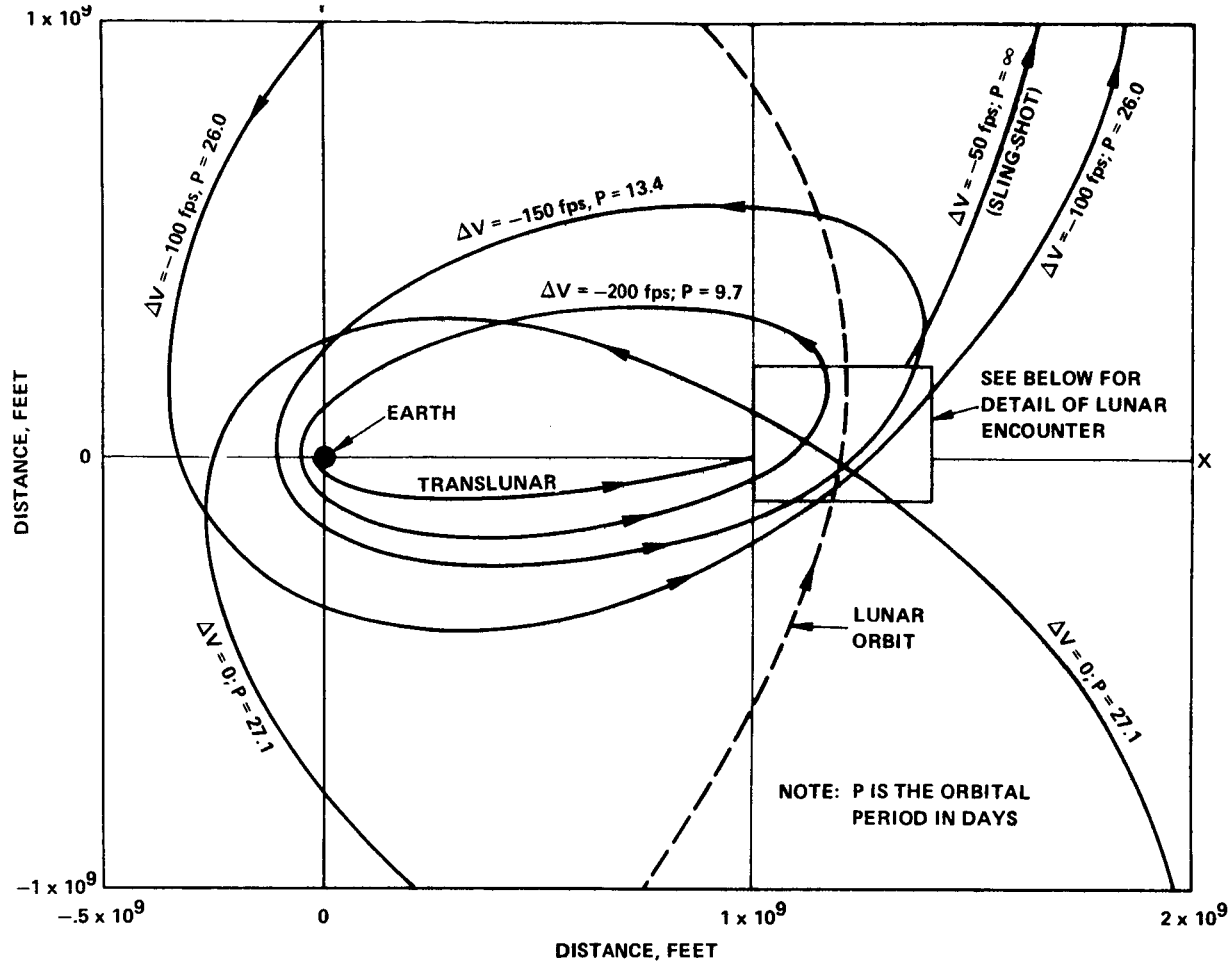

FIGURE 3a - GEOCENTRIC S-IVB TRAJECTORIES

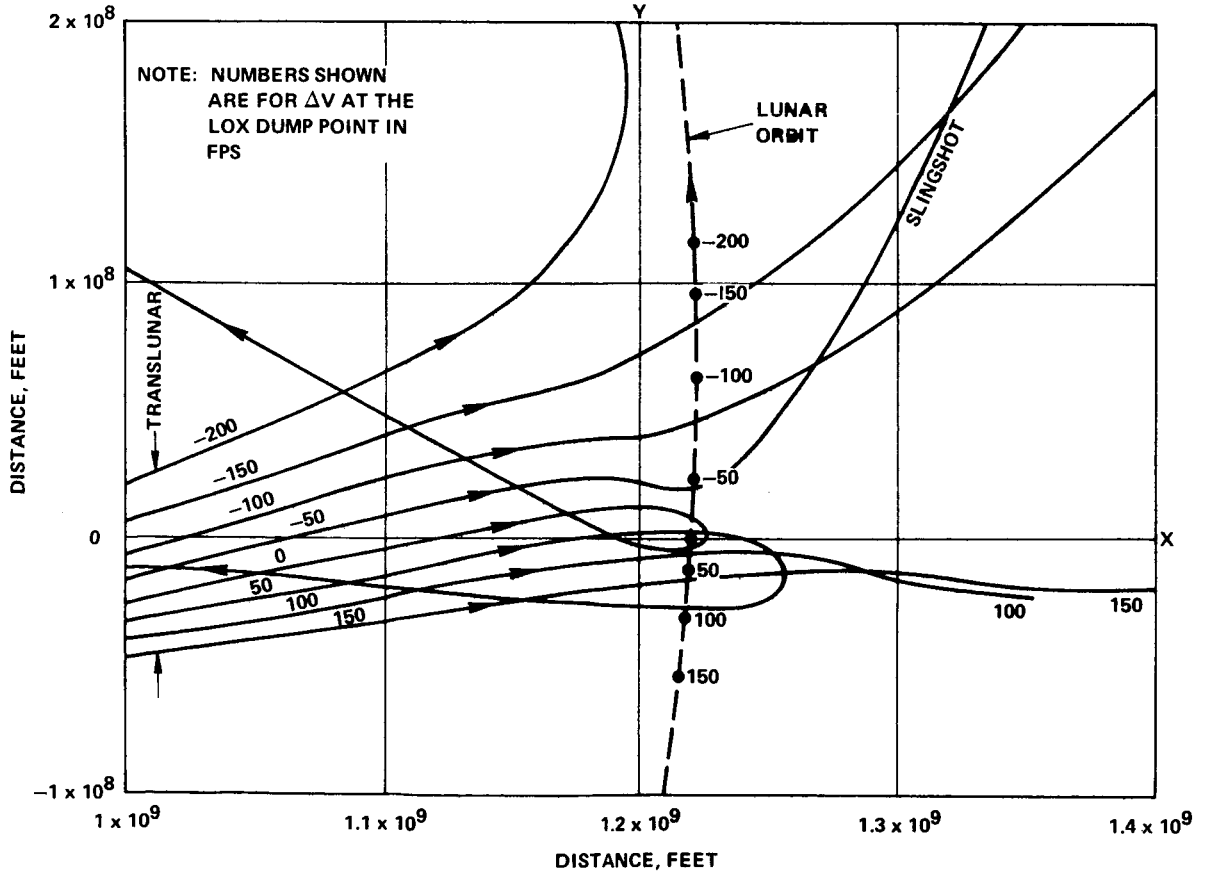

FIGURE 3b - DETAIL OF ENCOUNTER TRAJECTORIES

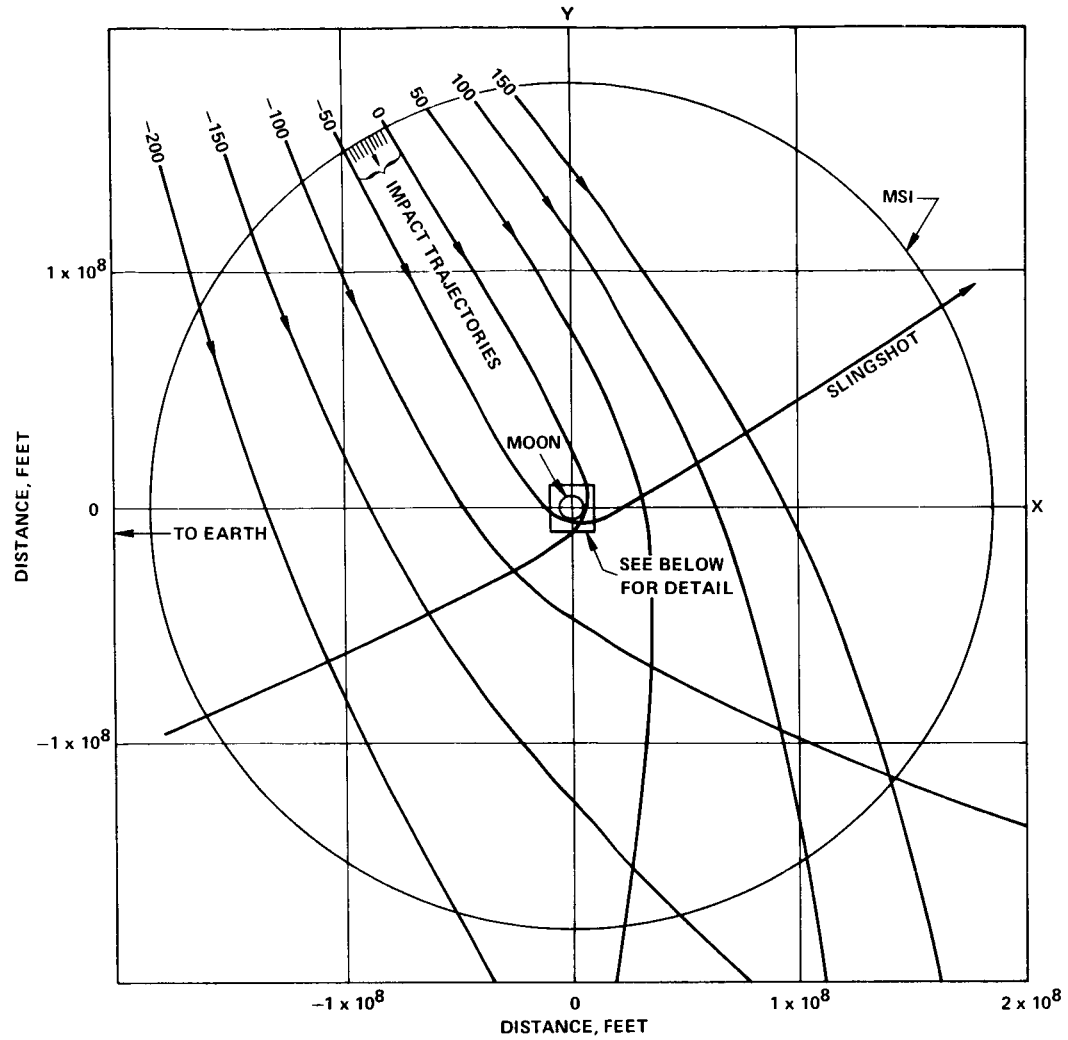

FIGURE 4a - SELENOCENTRIC S-IVB TRAJECTORIES

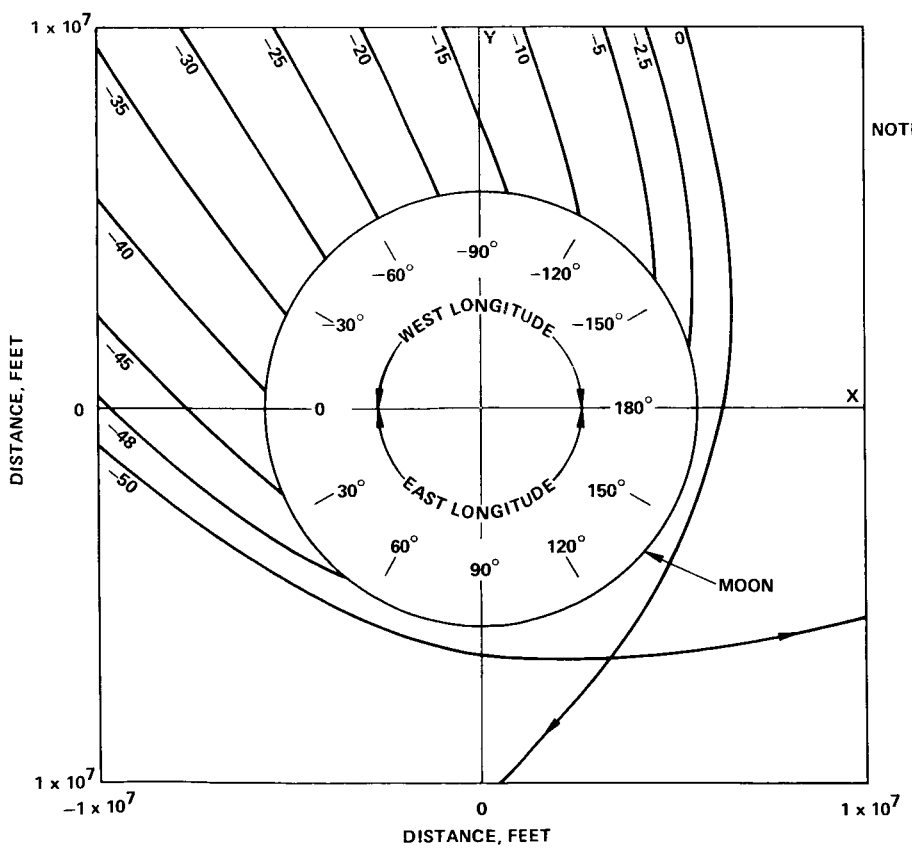

NOTE: NUMBERS SHOWN ARE FOR ΔV AT THE LOX DUMP POINT IN FPS

FIGURE 4b - DETAIL OF IMPACT TRAJECTORIES

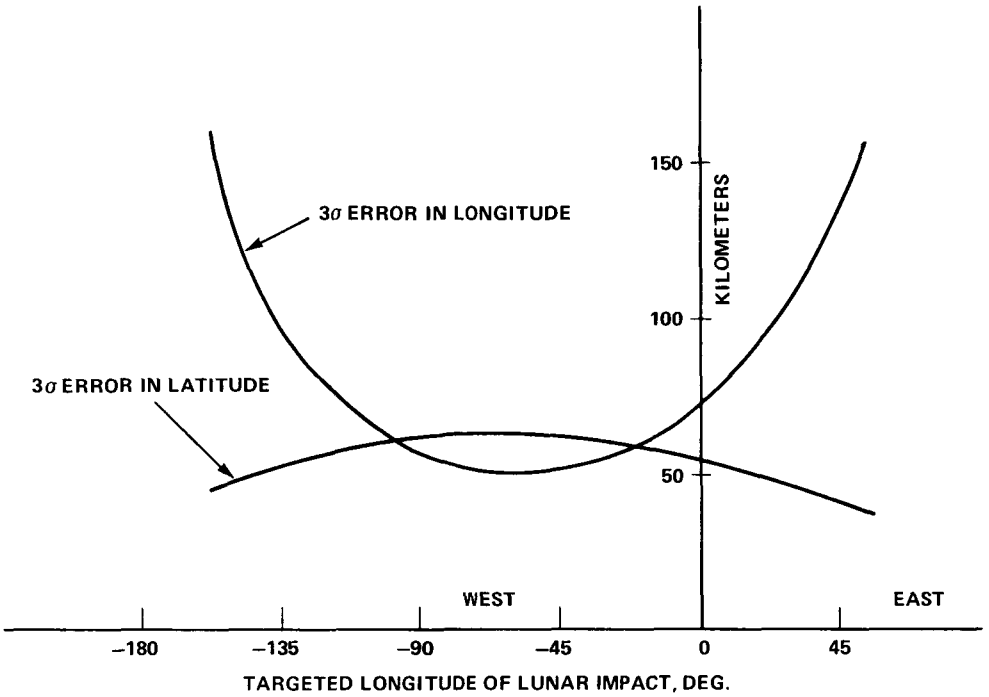

FIGURE 5a - VARIATION IN ERRORS WITH TARGETED LUNAR LONGITUDE
(TARGETED LATITUDE HELD CONSTANT AT 0°)

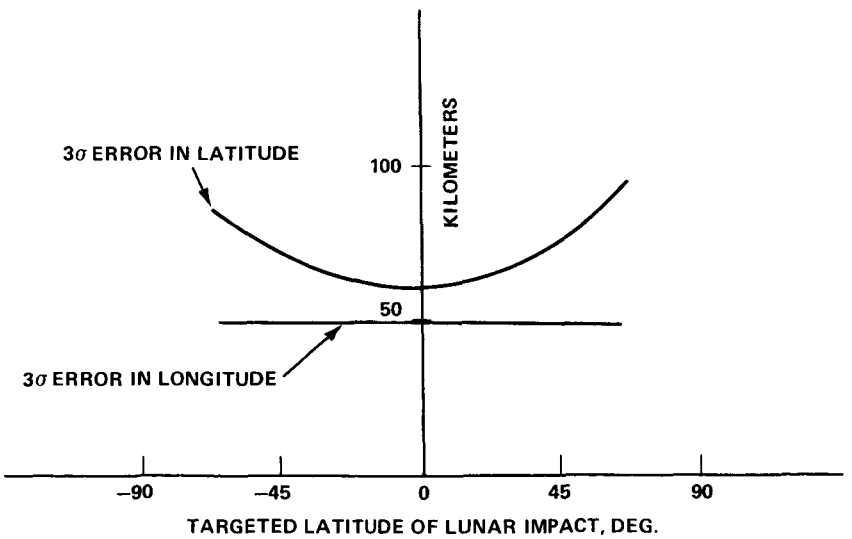

FIGURE 5b - VARIATION IN ERRORS WITH TARGETED LUNAR LATITUDE
(TARGETED LONGITUDE HELD CONSTANT AT –55°)

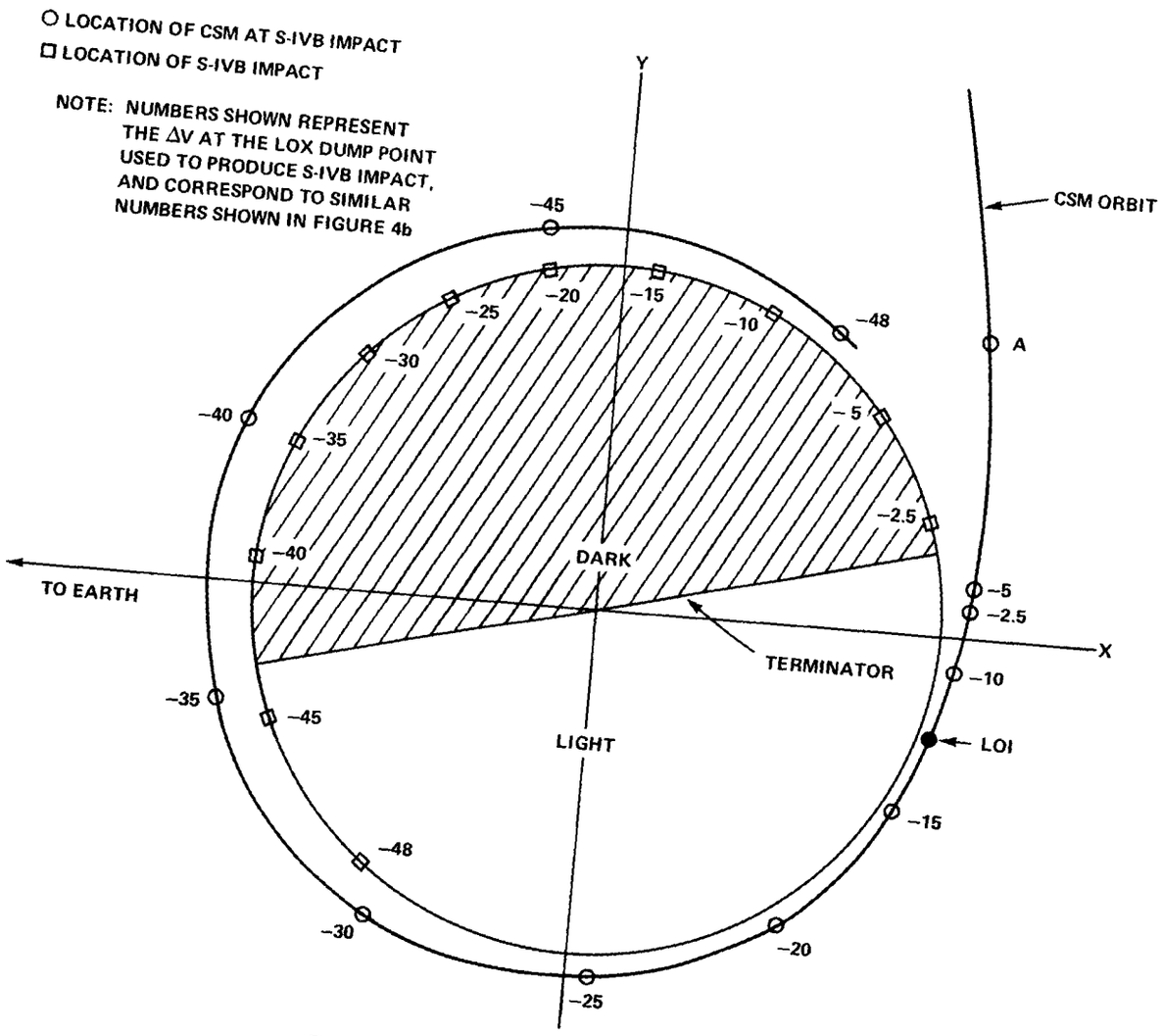

FIGURE 6 - VISIBILITY OF S-IVB IMPACT FROM THE CSM

Subject: Survey of Potential S-IVB Lunar Impact Trajectories for Apollo 16 and 17 -- Case 310

From: L. P. Gieseler

Distribution List

NASA Headquarters

J. K. Holcomb/MAO
C. M. Lee/MA
A. S. Lyman/MR
W. T. O'Bryant/MAL
R. A. Petrone/MA
W. E. Stoney/MAE

Manned Spacecraft Center

R. L. Berry/FM5
R. H. Kohrs/PD7
R. K. Osburn/FM4
C. W. Pace/FM13
G. W. Ricks/FM5
D. Segna/PD7
J. R. Sevier/PD4

Marshall Space Flight Center

R. E. Beaman/PM-SAT-E
W. D. McFadden/S&E-AERO-MMA
C. L. Thionnett/S&E-C&E-I

Lamont-Doherty Geological Observatory

G. V. Latham

University of Toronto

M. T. Yates

Bellcomm, Inc.

R. A. Bass
A. P. Boysen, Jr.
J. O. Cappellari, Jr.
F. El-Baz
D. R. Hagner

Bellcomm, Inc. (Continued)

W. G. Heffron
N. W. Hinners
T. B. Hoekstra
M. Liwshitz
K. E. Martersteck
J. Z. Menard
P. E. Reynolds
J. W. Timko
R. L. Wagner
All Members Department 2013
Central Files
Department 1024 File ← COPY TO
Library

Abstract Only to

Bellcomm, Inc.

J. P. Downs
I. M. Ross
M. P. Wilson